SCIENCE CHINA
Earth Sciences

•RESEARCH PAPER•

October 2022 Vol.65 No.10: 1847–1860
https://doi.org/10.1007/s11430-022-9975-0

Extreme large-scale atmospheric circulation associated with the "21·7" Henan flood

Jun XU[1], Rumeng LI[2], Qinghong ZHANG[2*], Yun CHEN[1†], Xudong LIANG[3] & Xiujie GU[4]

[1] *National Meteorological Center of China, Beijing 100081, China;*
[2] *Department of Atmospheric and Oceanic Sciences, School of Physics, Peking University, Beijing 100871, China;*
[3] *State Key Laboratory of Severe Weather, Chinese Academy of Meteorological Sciences, China Meteorological Administration, Beijing 100081, China;*
[4] *Henan Meteorological Observatory, Zhengzhou 450003, China*

Received January 25, 2022; revised June 12, 2022; accepted July 4, 2022; published online September 7, 2022

Abstract From July 19 to 21, 2021, Henan, a province in northern China (NC), was affected by severe flooding (referred to hereafter as "21·7") caused by a prolonged record-breaking extreme precipitation (EP) event. Understanding the extremes of the large-scale circulation pattern during "21·7" is essential for predicting EP events and preventing future disasters. In this study, daily atmospheric large-scale circulations over NC in the summers from 1979 to 2021 were investigated using the circulation classification method of an obliquely rotated principal component analysis in T-mode (PCT). The geopotential heights at 500 hPa and 925 hPa were applied successively in classification. Among the nine summer circulation patterns found at 500 hPa, the three days of "21·7" belonged to the Type 8 pattern, which had the second highest probability of EP days among all patterns. It was characterized by a southeasterly wind toward North China Plain driven by a dipole geopotential height field, with the West Pacific subtropical high (WPSH) extending far north to 30°N and low pressure to the south near NC. Tropical cyclones (TCs) occurred on 72.5% of EP days, in which larger amounts of precipitation and a longer duration of EP days were found along the mountains in NC, as compared with other patterns. The distribution of EP events under this pattern was mainly influenced by the location of the low pressure at 925 hPa in the dipole. The subtype 8-3 circulation, with low pressure in the east of Taiwan Island, included "21·7" and accounted for 1.6% of all summer days. Typhoon In-fa, together with the WPSH, gave rise to intense column integrated moisture flux convergence (IMFC) via the southeasterly wind to Henan, which occurred continuously during the 3 days of "21·7", resulting in the largest (second largest) mean IMFC among 3 consecutive EP days under type 8 (all types) during the past 43 summers in NC. Further analysis revealed that the large-scale dynamic process could not completely explain the record-breaking EP during "21·7", indicating possible contributions of other dynamic processes related to meso-scale convective storms.

Keywords Flood, Extreme precipitation, Large-scale circulation pattern

Citation: Xu J, Li R, Zhang Q, Chen Y, Liang X, Gu X. 2022. Extreme large-scale atmospheric circulation associated with the "21·7" Henan flood. Science China Earth Sciences, 65(10): 1847–1860, https://doi.org/10.1007/s11430-022-9975-0

1. Introduction

Henan Province, located in northern China (NC), experienced three consecutive days of extreme precipitation (EP) with record-breaking daily accumulated precipitation at 20 national operational weather stations from July 19 to 21, 2021 (Figure 1; referred to as "21·7" hereafter). Maximum hourly rainfall of 201 mm and daily precipitation of 624 mm were observed at the Zhengzhou weather station on July 20, 2021 (Yin et al., 2022). There were nine stations with 3-day precipitation reaching 500 mm in Henan (Figure 1). The EP led to floods, urban water logging, debris flows, and house

* Corresponding author (email: qzhang@pku.edu.cn)
† Corresponding author (email: chenyun@cma.gov.cn)

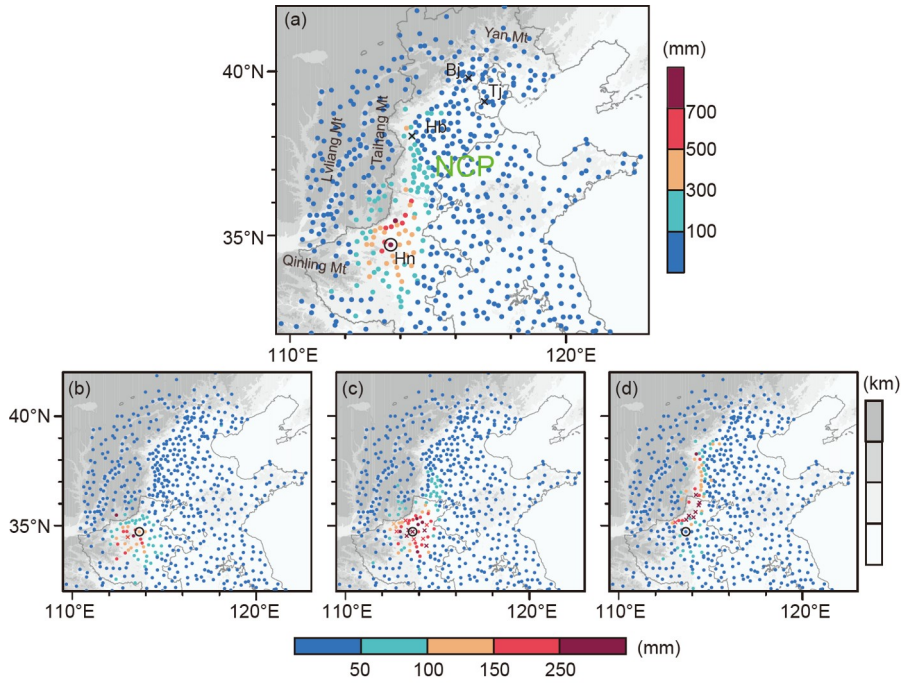

Figure 1 Accumulated precipitation from (a) 0800 LST July 19 to 0800 LST July 22, (b) 0800 LST July 19 to 0800 LST July 20, (c) 0800 LST July 20 to 0800 LST July 21, and (d) 0800 LST July 21 to 0800 LST July 22. Crosses in (b)–(d) indicate that precipitation at the station reached a historical maximum daily amount in the summers of 1951–2021. Hebei (Hb), Beijing (Bj), Henan (Hn), and North China Plain (NCP) are shown. Gray shading denotes the terrain height. The mountains are marked. The black circle shows the location of the Zhengzhou rain gauge station. The cross marks from north to south denote Beijing, Tianjin, and Shijiazhuang, respectively.

collapses, and caused 398 deaths and an economic loss of 120.06 billion RMB Yuan, according to a government disaster report (Disaster Investigation Team of The State Council of China, http://www.gov.cn/xinwen/2022-01/21/content_5669723.htm). Northern China has frequently been subject to urban water logging and flash floods due to EP during summer in recent years, including EP events in Beijing on July 21, 2012, and July 16, 2018, and in Hebei province on July 19, 2016 (Zhou et al., 2013; Zhang et al., 2013; Xia and Zhang, 2019; Cao et al., 2020). As the Yan, Taihang, and Qinling Mountains run along the northern and western parts of NC, according to 2020 statistics, the human population is concentrated on the plains parallel to the mountains (National Bureau of Statistics of China, data.stats.gov.cn). Most of the cities except Tianjin along the Taihang and Yan mountains in the North China Plain (NCP) have populations exceeding 5 million, and four cities (Zhengzhou, Beijing, Tianjin, and Shijiazhuang) have populations exceeding 10 million. Interestingly, all four cities are near the delta region (Figure 1a). The topography may facilitate the initiation and maintenance of mesoscale convection bringing intense precipitation through lifting or mountain-valley circulation processes with the summer monsoon circulation (Yin et al., 2011; Zhong et al., 2015; Pan and Chen, 2019); thus, affecting the safety of the human population and the economy in NC. It is, therefore, necessary to obtain a better understanding of when and where EP events in NC have occurred and will occur in the future.

Extreme precipitation can be associated with daily large-scale circulations (Liu et al., 2016; Zhao et al., 2019; Davenport and Diffenbaugh, 2021). It has been reported that the sources of uncertainty in climate projections are largely due to large-scale circulations (e.g., Shepherd, 2014; Zappa et al., 2015). Additionally, EP events are often correlated with convective storms (e.g., Dowdy and Catto, 2017; Ng et al., 2022; Zhao, 2022) and large-scale circulation could result in conditions favorable for the occurrence of convection. Therefore, an investigation of the daily large-scale atmospheric circulations associated with EP events may improve our understanding of key dynamic factors related to EP, which would be helpful for predicting EP events. Climate warming and urbanization will lead to more frequent and intense EP in the summer monsoon region, including NC (Wang et al., 2021). Clarifying the types of circulation that are conducive to EP in NC in summer is crucial for both a scientific understanding and preventing disasters.

Previous research on large-scale circulation-related to EP in NC has included composite and case studies. A composite analysis revealed several circulation patterns associated with EP in NC, including meridian circulation with a northward and westward extended West Pacific subtropical high (WPSH) (Tao et al., 1980; Ding and Chan, 2005; Zhao et al., 2013; Zhao et al., 2019), warm (cold) anomalies in the upper-level troposphere (Sun et al., 2015), large-scale frontal

systems, and weakened landfall tropical cyclones (TCs) (Zhou et al., 2020). However, none of these patterns corresponded to the circulation of "21·7", with a TC far from the East China Sea (Yin et al., 2022), suggesting that such EP events may be relatively low-probability events missed by previous composite analyses. The large-scale circulation characteristics of this EP event and its precipitation characteristics, such as the intensity and duration, are largely unknown.

Case studies related to EP in NC have revealed that a low vortex (Liao et al., 2013), the combined effects of a subtropical high and upper trough (Cao et al., 2020), low level jet, extratropical cyclogenesis, and topography lifting (Xia and Zhang, 2019) are conducive to EP in NC. These case studies demonstrated the diversity of individual circulations in EP events and were unable to reveal the common large-scale circulation characteristics that may be the key dynamic factors and signals in the projection and forecasting of EP events.

This study initially used the large-scale circulation patterns associated with EP in NC between 1979 and 2021 to determine the common key dynamic factors underlying each circulation pattern. It then sought to clarify whether the circulation related to "21·7" was extreme.

2. Data and methods

2.1 Observation and reanalysis data

Summer was defined as the period from June 1 to August 31. Daily accumulated precipitation data were collected from 08:00 LST (local solar time) to 08:00 LST of the next day from the 617 national meteorological operational rain gauge stations in NC. Data were obtained from the National Meteorological Information Center of the China Meteorological Administration (CMA; http://data.cma.cn/) and subjected to quality control. Data from stations missing more than 10% of records in the 43 summers from 1979 to 2021 were removed, and the remaining data of 579 stations were used to study precipitation extremes (Figure 1).

The fifth generation of the European Centre for Medium-Range Weather Forecasts atmospheric reanalysis data of the global climate (ERA5) (Hersbach et al., 2020; https://cds.climate.copernicus.eu/) at 08:00 LST with a latitude-longitude grid of 0.25° resolution and 37 vertical levels was used in a circulation analysis to investigate precursor circulations. In calculations of the daily mean and accumulated column integrated moisture flux convergence (IMFC), hourly data from 08:00 to 07:00 LST of the next day were applied.

Hourly precipitation data from 932 hydrological and 10,352 meteorological rain gauge stations was used to generate daily gridded precipitation data from July 19 to 21, 2021 with a latitude–longitude grid of 0.01° resolution in the region of 30°–38°N, 109°–117°E. Hourly and daily data from each station were compared with the data from surrounding stations. Stations with abnormal data were excluded as a quality control procedure. Grid data with a horizontal resolution of 0.01° were generated by the Cressman interpolation method (Cressman, 1959), with the radius of influence being reduced from 0.18° to 0.02°. The grid data were used for verification of ERA5 daily precipitation.

Advanced time of arrival and direction system (ADTD) lighting location data from July 19 to July 21 2021 obtained from the China Meteorology Administration was used in the thunderstorm analysis. The data included the time, location and polarity of the lightning (Hu et al., 2018; Yao et al., 2012). The location of the lighting was used in this study.

To analyze the TC activities in each type of summer circulation, the CMA Tropical Cyclone Best Track Dataset from 1979 to 2020 (tcdata.typhoon.org.cn; Ying et al., 2014; Lu et al., 2021) with 6-h intervals was applied. The track data of Typhoon In-fa in 2021 were obtained from the National Meteorological Center. For any given day, TC track data from 08:00 to 08:00 LST the next day were collected and only those with tracks in the region 15°–55°N, 95°–145°E were considered.

2.2 Definition of EP days and dry days

Considering that 100 mm was the criterion for torrential rain according to the Operational Weather Forecast Agency in China and the intensity of the 99.9th percentile daily precipitation was no less than 100 mm at 81.5% of rain gauges in NC (Figure 2a), daily precipitation no less than 100 mm was defined as an EP event for each station between 1979 and 2021. Daily precipitation of 100 mm was within the top third-percentile daily precipitation at all stations in NC (Figure 2b). Continuous EP events were defined as no less than two consecutive days of EP events at any given station. Considering the social impact of precipitation extremes within certain areas, EP days were defined as days in which EP events were recorded at a minimum of five stations. In contrast, dry days were defined as days in which no stations recorded precipitation above 25 mm in NC, which is the criterion for heavy rain according to the Operational Weather Forecast Agency in China. Applying these criteria, 374 EP days and 613 dry days were identified in the 3956 summer days from 1979 to 2021.

2.3 Circulation classification method

An obliquely rotated principal component analysis (PCA) in T mode (PCT) (Huth, 1993, 1996a, 1996b, 2000) was applied to classify atmospheric circulation patterns. This

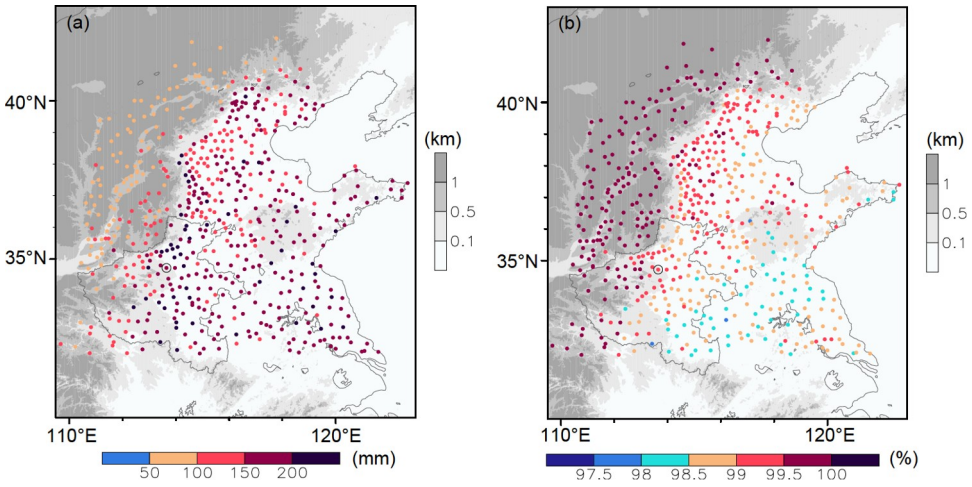

Figure 2 (a) Spatial distribution of the 99.9th percentile of daily precipitation intensity in summer and (b) the percentiles of 100 mm daily summer precipitation from 1979 to 2021. The black circle shows the location of the Zhengzhou rain gauge station.

method has been used successfully in previous studies of atmospheric circulation patterns associated with several weather phenomena in China, such as the EP in spring in NC (Xu et al., 2022, mesoscale convective systems in central China (He et al., 2017), and hailstorms across the country (Li et al., 2016), yielding stable results and explicit physical explanations. To gain an objective overview of the atmospheric circulations corresponding to EP days over the past 3956 summer days and to avoid false interpolation under topography, 500 hPa geopotential heights, which can result in more realistic and physically significant flow patterns in summer, were applied in the classification. The classification area was in East Asia (15°–55°N, 95°–145°E). A further circulation classification at a geopotential height of 925 hPa was conducted in an NC region (30°–42°N, 110°–122°E) with the same circulation type as "21·7".

3. The circulation pattern and its physical explanation

Consistent with the recommended method of determining circulation types (Huth, 1996b, 2000), daily circulations in East Asia were classified in to nine types that could explain 83.2% variance of the 500 hPa geopotential heights in the past 43 summers. In addition to the circulation characteristics and EP event spatial distributions of the circulation type related to "21·7", other leading circulations of EP days in NC were also investigated.

3.1 Circulation types and related EP event distributions in NC

According to the classification results, all days during the period July 19–21, 2021 were classed as Type 8, which was characterized by a dipole geopotential height field with a low in southern China and a high in the adjacent seas of northeast Asia (Figure 3h). The high extended to northeast China at high latitudes. The transition zone between the high and low was associated with southeasterly wind from the East China Sea at 850 hPa to NC (Figure 3h). The WPSH ridge line was defined as the line within the range of 5880 gpm at 500 hPa, where the zonal wind speed (u) was zero and the meridional gradient of u was above zero (Liu and Wu, 2004; Mao et al., 2020). The location of the WPSH ridge line of Type 8 circulation was at ~30°N, which was the northernmost location among all nine circulation types (Figure 3). A correspondingly high frequency of EP events was distributed along the mountains in the NCP, especially in the delta topography region in Henan, Hebei Province, and Beijing (Figure 4h). Especially high frequencies of extraordinary rainstorms (daily precipitation ≥250 mm) were distributed in the NCP along the Qinling Mountains and Yan Mountains (Figure 4h). A high frequency of EP events was also distributed in the eastern part of the NCP, with a wide spatial distribution. Although Type 8 circulation accounted for a small proportion (8%) of all days in summer, it had the second highest probability (13.6%) of EP days after Type 5 circulation (Figure 5a). Additionally, Type 8 circulation EP days had a continuous characteristic, with 40% occurring on 2 or more consecutive days, which was the highest proportion among the nine types (Figure 5a). The precipitation amount of EP events was also highest for Type 8 among the nine types, with the largest median, 75th percentile, 90th percentile, and maximum values (Figure 5b).

In addition to Type 8 circulation, three other types of circulation (Type 1, Type 5, and Type 6) with the WPSH ridge line north to 25°N contributed 62.3% of the EP days (Figure 3a, 3e and 3f). These were the top three leading circulations contributing to EP days, while Type 2, Type 4, and Type 7,

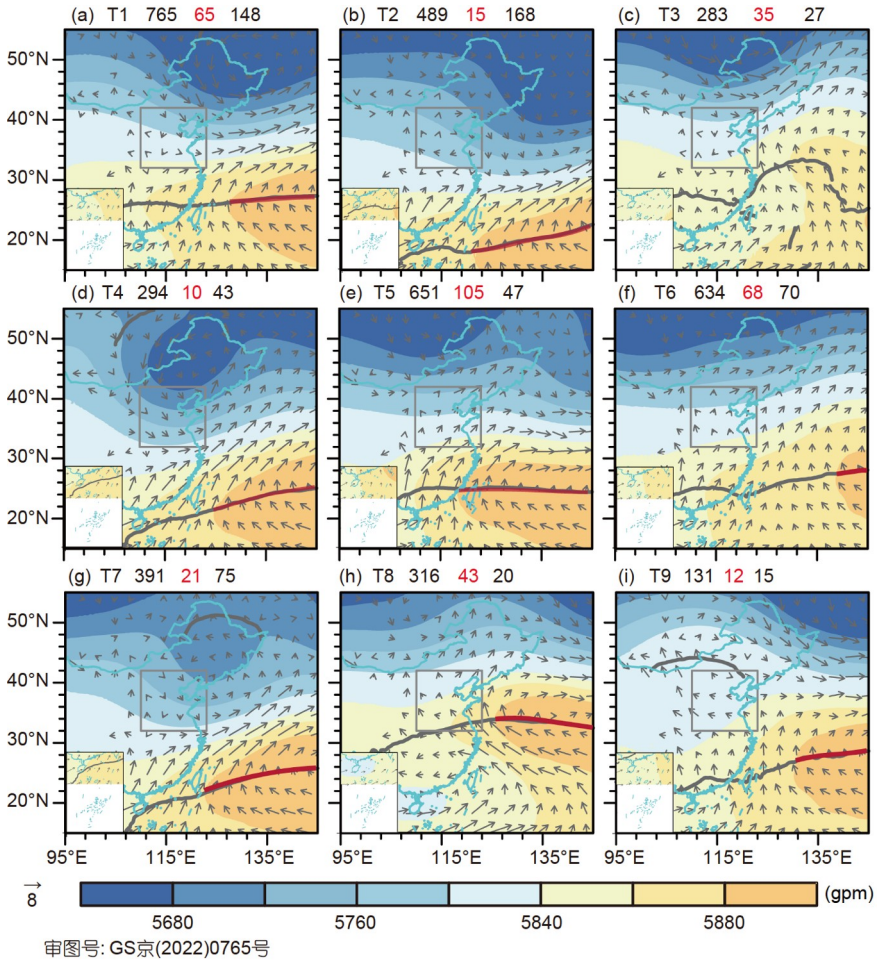

Figure 3 Mean geopotential height (shadings) and zero zonal wind speed lines at 500 hPa (dark grey lines; red lines are the ridge lines of the West Pacific subtropical high), and for horizontal winds at 850 hPa (vectors; unit: m s^{-1}) for the nine circulation types in the summers from 1979 to 2021. The three numbers at the left top of each panel are the numbers of total days, extreme precipitation (EP) days, and dry days for each circulation type, respectively.

with WPSH ridge points south of 25°N, only contributed 12% of EP days in NC (Figure 5a). Type 1 is a type of Meiyu circulation pattern (He et al., 2017), in which low pressure was prevalent in NC. The ridge line of the WPSH was located at ~25°N (Figure 3a). Extreme precipitation events with extraordinary rainstorms and continuous EP events were frequently distributed in the southern NC under Type 1 circulations (Figure 4a). Accounting for most of the EP days in NC, Type 5 circulations had the most westward extended subtropical high and low pressure covered eastern Mongolia (Figure 3e). Type 5 was a meridional circulation (Tao et al., 1980) with southwesterly wind prevailing in the eastern part of NC. The EP days under Type 5 were frequently distributed in the eastern parts of NC (Figure 4e), while EP events with extraordinary rainstorms were frequently distributed in the NCP along the Yan Mountains and Taihang Mountains. Continuous EP events were frequently distributed in southern NC under Type 5 circulations (Figure 4e). The circulations of EP events on July 21, 2012, and July 19, 2016, were classified as Type 5. Compared with Type 5 circulations, the low pressure in Mongolia associated with Type 6 circulations was further north and the WPSH under Type 6 circulations was further east, leading to a weaker southwesterly wind in the eastern part of NC (Figure 3f). Accordingly, the frequency of EP events under Type 6 circulations was lower than under Type 5 circulations, and EP events were prone to occur in the NCP along the mountains (Figure 4f).

Although Type 1, Type 5, and Type 6 circulations contributed more EP days than Type 8 circulation, only 26%, 25%, and 29% of EP days under Type 5, Type 6, and Type 1 circulations were continuous, while the corresponding rate under Type 8 circulation was 40% (Figure 5a). Additionally, EP events with extraordinary rainstorms and continuous EP events under Type 8 were distributed in the NCP along the mountains in NC, especially in the delta topography regions in Henan, Hebei, and Beijing (Figure 4h).

In summary, compared with the leading EP day circulations of Type 1, Type 5, and Type 6 circulations, all of which were characterized by southwesterly winds in lower troposphere, Type 8 circulation, which was characterized by strong southeasterly wind, was more likely to produce continuous EP days or EP events with large amounts of pre-

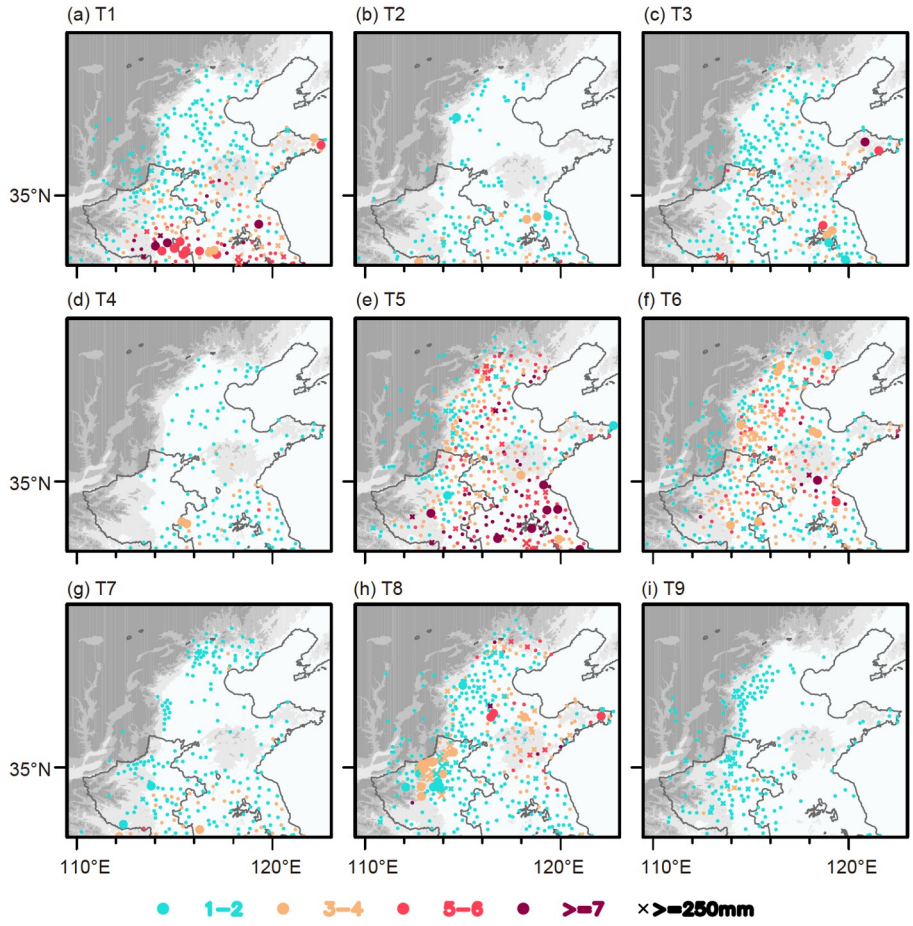

Figure 4 Color-coded frequencies of EP events under each circulation type. Stars mark the stations where extraordinary rainstorms (daily precipitation exceeding 250 mm) occurred at least once. Large marks indicate stations where continuous EP events occurred at least once. Grey shade represents the terrain height. Light grey shading indicates elevation higher than 500 m but lower than 1,500 m. The dark grey shaded areas represent elevation over 1,500 m.

cipitation along the mountains in the NCP, especially in the delta region.

3.2 Common large-scale dynamic processes related to EP days under Type 8 circulation

Although Type 8 circulation promoted EP days in NC, only 13.6% of days under Type 8 circulation were EP days, indicating the diversity of circulation. It was therefore considered important to determine if differences existed between EP days and dry days under Type 8 circulation.

In the dipole geopotential height field, the high and low pressures on EP days were stronger than average (Figure 6a and 6c). The WPSH was significantly stronger and extended further westward to NC, leading to stronger pressure gradients in the area from the East China Sea to NC, supporting a stronger southeasterly wind at lower levels. This resulted in a significantly stronger southerly wind from the East China Sea to NC at low altitudes, bringing more moisture and warm air with a higher equivalent potential temperature to NC on EP days (Figure 6a, 6c and 6d). The WPSH was further eastward on dry days in comparison to EP days (Figure 6c). Although dipole geopotential height fields were also identified, they were in a different location on EP days. Large pressure gradients were observed in the East China Sea, while NC was dominated by northeasterly winds at 850 hPa (Figure 6c) on dry days.

To qualify the moisture transport by the significantly strong southerly winds under Type 8 circulation, we also composited the vertically integrated water vapor transport (IVT), which is defined as:

$$\mathrm{IVT} = \frac{1}{\mathrm{g}} \int_{p_{\mathrm{sfc}}}^{p} q\,\mathbf{V}\mathrm{d}p, \tag{1}$$

where g is the acceleration due to gravity, q is the specific humidity, $\mathbf{V}$ is the horizontal wind, p_{sfc} is the surface pressure, and p was set to 300 hPa.

The IVT on EP days was significantly stronger than the average in NC (Figure 7a, 7c, and 7d). A large IVT center, with a maximum IVT > 500 kg m^{-1} s^{-1}, occurred from the East China Sea to NC, bringing abundant moisture to NC (Figure 7a). However, EP events were mainly distributed

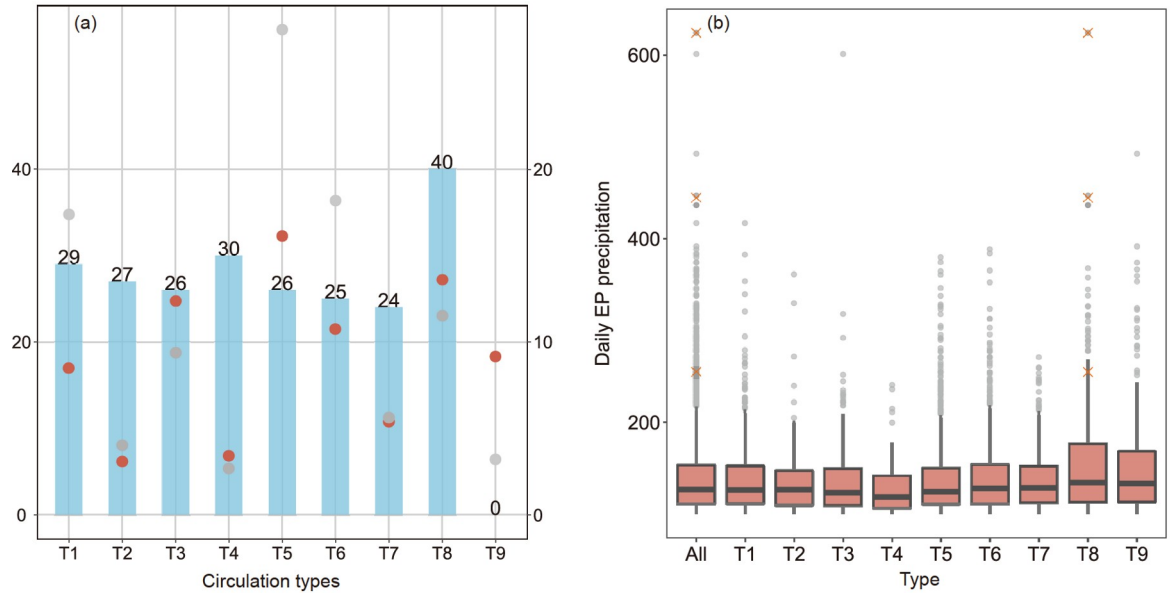

Figure 5 (a) Proportion of consecutive EP days relative to the total EP days for each type of circulation pattern (blue bar, unit: %). Red dots indicate the proportion of EP days relative to the total EP days for each circulation pattern (right axis, unit: %). Gray dots indicate the proportions of EP days under the different circulation patterns relative to the total summer EP days (right axis, unit: %). (b) Boxplots of daily precipitation during EP events for each circulation pattern. The orange x symbol marks indicate the maximum daily precipitation during July 19–21, 2021.

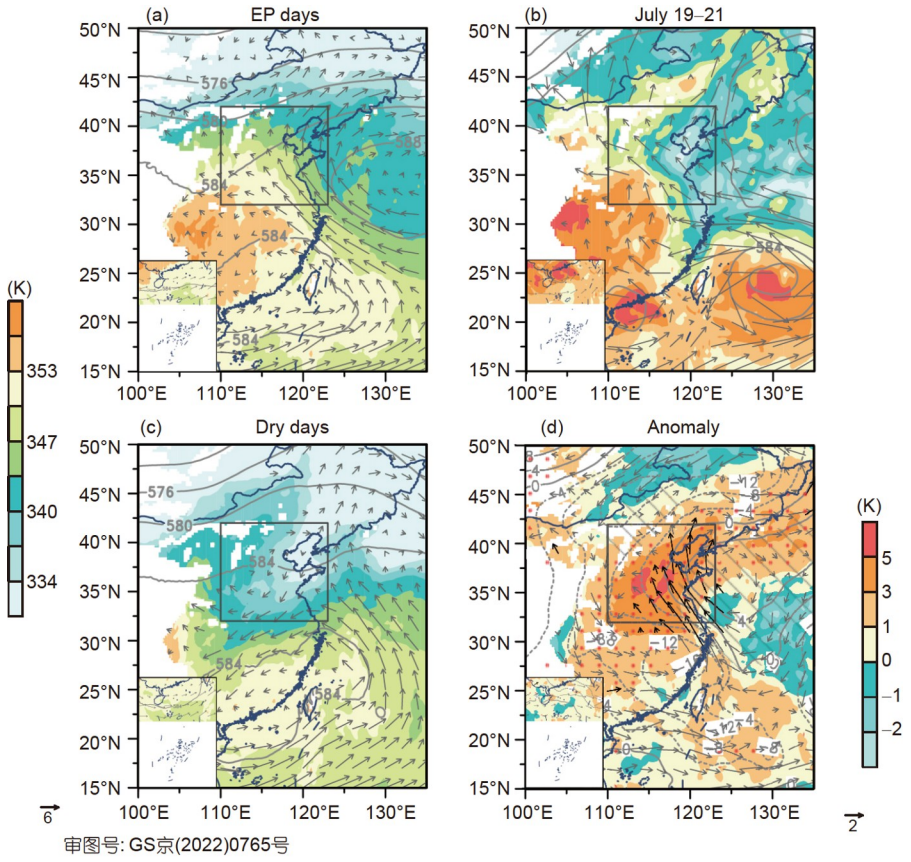

Figure 6 Composite analysis of EP days (left color bar) (a), July 19–21, i.e., "21·7" (left color bar) (b), dry days (left color bar) (c) and the anomaly of EP days (right color bar) (d) under Type 8 circulation days. Equivalent potential temperature at 850 hPa (shading) and 500 hPa geopotential heights (contours; unit: 10 gpm), and for horizontal winds at 850 hPa (vectors). Black vectors indicate the difference in meridional wind between EP days and all Type 8 circulation days exceeding the 95% confidence level. Geopotential height is denoted by slashed lines. Red dots indicate the equivalent potential temperature. The study region is indicated by the grey rectangle (32°–42°N, 110°–123°E).

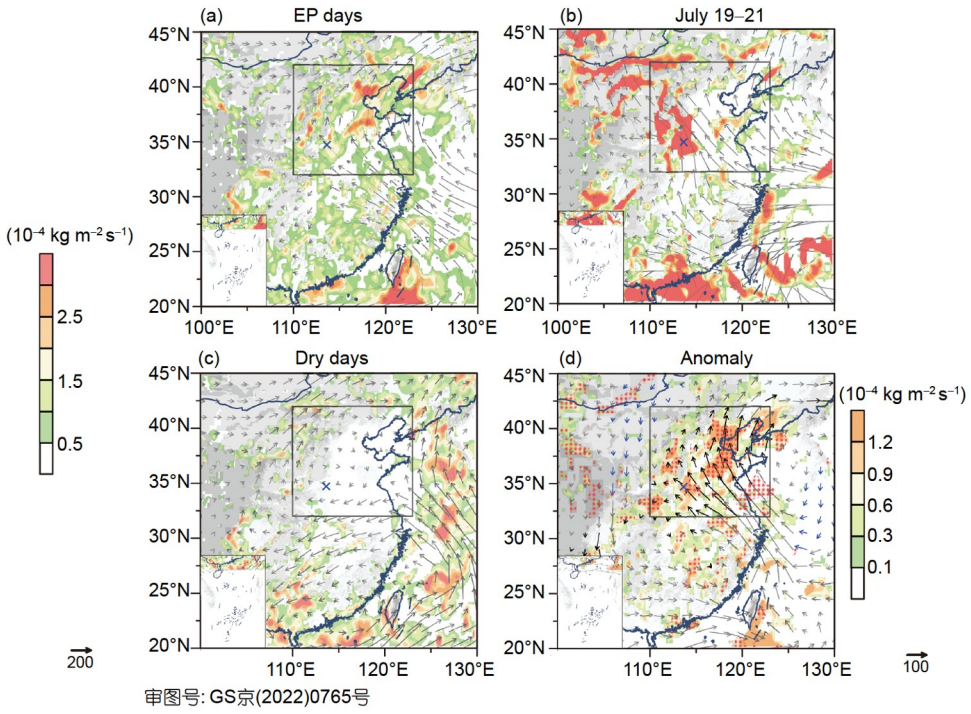

Figure 7 Same as Figure 6, but for integrated water vapor transport (IVT) vectors and the integrated moisture flux convergence (IMFC). Shading represents (a)–(c) an integrated IMFC greater than 0.5×10^{-4} kg m^{-2} s^{-1}. Black vectors indicate the difference in the magnitude of IVT between EP days and all Type 8 circulation days exceeding the 90% confidence level. Red dots indicate the IMFC. The blue cross shows the location of Zhengzhou. The study region is indicated by the grey rectangle (32°–42°N, 110°–123°E). Grey shade represents the terrain height. Light grey shade indicates elevation higher than 500 m but lower than 1,500 m. The dark grey shading represents areas with elevation over 1,500 m.

in the NCP along the mountains and eastern NC, suggesting that there may be more key large-scale dynamic factors related to EP events under Type 8 circulation, such as topographic lifting and atmospheric dynamic convergence.

According to the conservation of water vapor in pressure coordinates (Banacos and Schultz, 2005):

$$\overline{P}-\overline{E}=-\frac{1}{\mathrm{g}}\int_0^{p_{\mathrm{sfc}}}\frac{\partial q}{\partial t}\mathrm{d}p-\frac{1}{\mathrm{g}}\int_0^{p_{\mathrm{sfc}}}\nabla\cdot(q\mathbf{V})\mathrm{d}p, \tag{2}$$

where P is precipitation, E is evaporation, and the overbar represents a vertically integrated quantity. If evaporation is small in areas of intense precipitation and saturation, the above equation could be simplified as:

$$\overline{P}+\frac{1}{\mathrm{g}}\int_0^{p_{\mathrm{sfc}}}\frac{\partial q}{\partial t}\mathrm{d}p\approx-\frac{1}{\mathrm{g}}\int_0^{p_{\mathrm{sfc}}}\nabla\cdot(q\mathbf{V})\mathrm{d}p, \tag{3}$$

where the term on the right hand side is the IMFC. In intensive precipitation, the term $\frac{1}{\mathrm{g}}\int_0^{p_{\mathrm{sfc}}}\frac{\partial q}{\partial t}\mathrm{d}p$, which is the local time variation of column integrated water vapor, is smaller compared to IMFC. Therefore, the IMFC is directly related to the local precipitation. Here, we calculated the IMFC from the surface to 300 hPa. A composite analysis (Figure 7a, 7c and 7d) revealed a significantly stronger IMFC in the NCP along the mountains in NC on EP days in comparison with the average and dry days, especially in the delta topography region in Henan, Hebei, and Beijing. The IMFC was also significantly stronger in the eastern part of NC (Figure 7d), which was consistent with the spatial distribution of EP events in Type 8 circulation (Figure 4h).

To understand how extreme the large-scale circulation during the "21·7" flood was, the composite average of the 3 days was analyzed (Figure 6b). A more northwestward extended WPSH and stronger low pressure extended from southwestern China to NC. The low associated with Typhoon In-fa, which was included in the composite average of the 3 days, was stronger than that on Type 8 EP days. There was a strong southeasterly wind in Henan Province and adjacent regions, which promoted the prolonged extreme IMFC (Figures 6b and 7b).

There were obvious circulation differences between EP and dry days under the same Type 8 circulation conditions, however, EP "hot spots" exist in several different locations, as shown in Figure 4h. We further categorized Type 8 circulation days into groups based on the 925 hPa geopotential height, to determine the dominant factor in the location diversity of EP events. Daily circulations in NC under Type 8 conditions were classified into five sub-types (Type 8-1, Type 8-2, Type 8-3, Type 8-4, and Type 8-5) that explained 97% of the variance in the 925 hPa geopotential height among 316 Type 8 circulation days.

The location of the low in the dipole differed among the five circulation sub-types (Figure 8). The lows under Type 8-

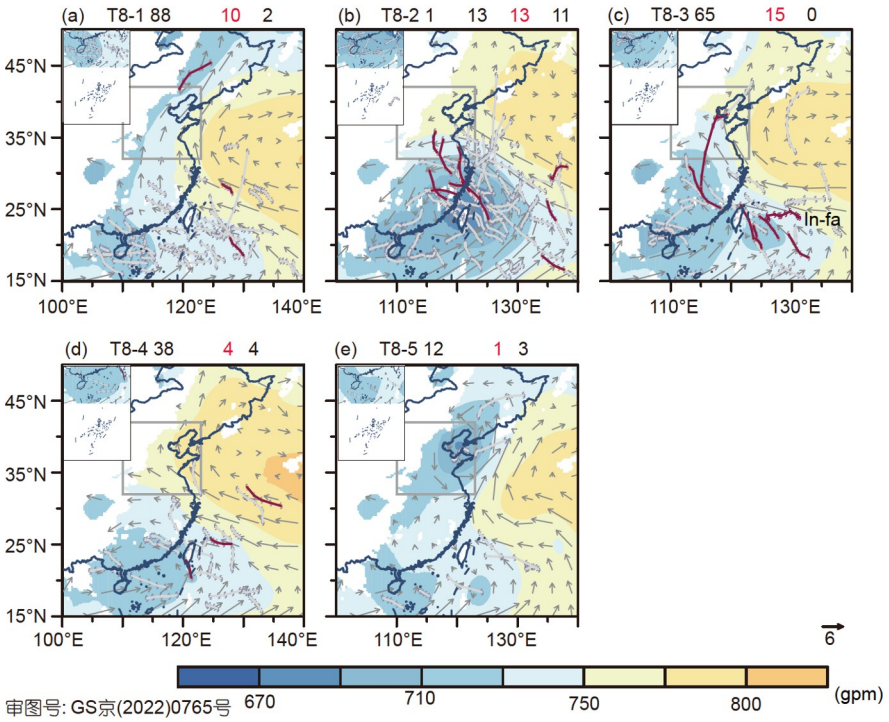

Figure 8 Mean geopotential height (shading) and horizontal wind at 925 hPa (vectors; unit: m s^{-1}) of the five sub-types of Type 8 circulation from 1979 to 2021 and tropical cyclone (TC) tracks on the days with each circulation type during 1979–2020. The three numbers at the top left of each panel are the numbers of total days, extreme precipitation (EP) days, and dry days for each circulation type, respectively. The TC tracks on EP days are marked in red. The track of Typhoon In-Fa from 0800 LST July 19 to 0800 LST July 22, 2021 is marked. The track data of Typhoon In-Fa were obtained from the National Meteorological Center of China.

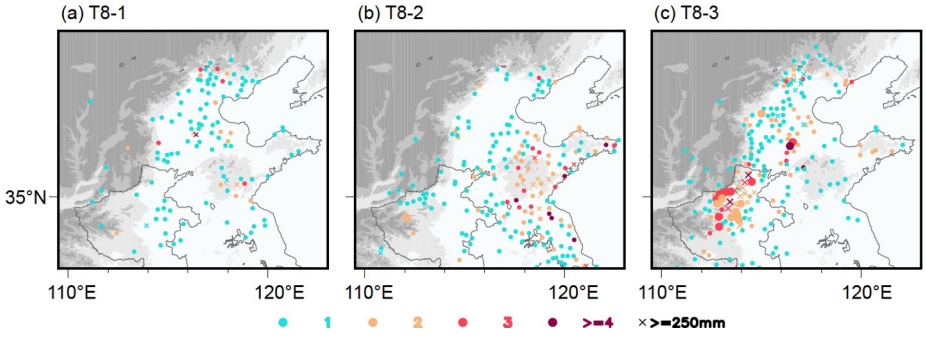

Figure 9 Same as Figure 4, but for the Type 8-1, Type 8-2, and Type 8-3 circulations.

2, Type 8-3, and Type 8-4 circulations were in the southern part of China and adjacent seas (Figure 8b–8d), while the lows under Type 8-1 and Type 8-5 circulations were to the west of the WPSH (Figure 8a and 8e). Type 8-1, Type 8-2, and Type 8-3 were the major circulation types on Type 8 circulation days, accounting for 88.4% of Type 8 circulation EP days and 84.2% of all Type 8 circulation days. Type 8-3 accounted for 34.9% of EP days under Type 8 circulation, and 23.1% of the Type 8-3 circulation days were EP days, which represented the largest proportions among the five sub-types. All 3 days of the "21·7" flood belonged to this type of circulation. Interestingly, this sub-type of circulation was most similar to the EP days of Type 8 circulation (Figure 6a) and there were no dry days. The low extended northeastward to NC, generating a southeasterly wind in the NCP. Another low geopotential height center was identified in the region east to Taiwan Island, and was accompanied by TCs (Figure 8c). Influenced by the topographic lift, EP events during this type of circulation frequently occurred along the mountains in the NCP, especially in the delta region in Henan, Hebei Province, and Beijing (Figure 9c). Type 8-2 circulation was characterized by a low centered in the region east of the southern China coastline, in which substantial TC activity occurred (Figure 8b), resulting in a strong southerly wind in the southeastern part of NC. Correspondingly, the frequent EP events in the eastern NCP (Figure 9b) were mainly caused by TC precipitation. Interestingly, this type of circulation accounted for 55% of the dry days under Type 8

circulation, making it the sub-type of circulation most similar to the dry day circulation under Type 8 conditions (Figure 6c). Type 8-1 circulation was characterized by a low in the western NC and a southerly wind. It was also influenced by lifting due to the topography, and EP events frequently occurred in the northern NCP along the Yan Mountains (Figure 9a).

In summary, compared to the dry days and the average, EP days under Type 8 circulation had a stronger dipole and significantly stronger southerly wind, bringing more moisture (which was essential for EP events). Different locations of the low in the dipole could lead to differences in the spatial distribution of the southerly wind; in turn, this could affect the spatial distribution of the IMFC, and therefore affect the location of EP events. Interestingly, mesoscale cyclone circulation was detected in the southwestern NC in the 850 hPa anomaly wind field (Figure 6d), consistent with the mesoscale vortex circulation near Henan (Yin et al., 2022) during "21·7". This suggested that the mesoscale vortex may be formed by some common physical processes under Type 8 circulation; thus, the "21·7" circulation was not unique. Further research will be required to characterize the formation of the mesoscale cyclone circulation.

3.3 Extreme characteristics of the large-scale circulation during the "21·7" flood

The daily mean IMFC at the grid nearest to the stations with EP events over the past 43 summers was calculated. Comparisons showed that the probability density of the daily mean IMFC of EP events was greater on Type 8-3 circulation days than on all summer and Type 8 circulation days when the daily mean IMFC was above 0.0013 kg m^{-2} s^{-1} (Figure 10). This was helpful for the EP events with large amounts of precipitation. The maximum 3-day mean IMFC in "21·7" for Henan and its adjacent region was 0.0014 kg m^{-2} s^{-1}, which was in the top 8.7th percentile for all EP events on summer days in the past 43 years (Figure 10), indicating prolonged extreme circulation during "21·7". The maximum mean IMFC during 3 consecutive EP days featuring one of the nine types of circulation in the past 43 summers were also calculated. The results showed that the maximum mean IMFC during "21·7" reach number 1 among all consecutive EP days (range: 0.0003 to 0.0009 kg m^{-2} s^{-1}) above 2 days. While it was number 2 among all consecutive EP days above 2 days in all summer days. The daily mean IMFC in 21 July 2021, with daily precipitation of 624 mm, at Zhengzhou weather station was 0.0015 kg m^{-2} s^{-1}, which was in the top 9.8th percentile for Type 8 circulation days and top 6.4th percentile for all summer days (Figure 10).

Whether the large scale and extreme circulation for "21·7" explains the record-breaking precipitation needed further investigation. In the 3-day period from July 19 to July 21, 2021, the 3-day IMFC was close to the ERA5 daily precipitation (Figure 11a–11f), also indicating that the IMFC calculated based on the ERA5 data could be a good large-scale key dynamic process parameter for EP days in NC. To compare the ERA5 and observed daily precipitation data, daily precipitation data with a 0.01° horizontal resolution was upscaled to 0.25°. However, the daily ERA5 precipitation was at least 200 mm lower than observed in the precipitation center on July 19–21, 2021 (Figure 11j–11l). Interestingly, these areas with severely underestimated precipitation were also accompanied by the most intense precipitation (>250 mm) and thunderstorms (Figure 11g–11i). Statistically, although the area-averaged ERA5 and upscaled observed daily precipitation amounts were comparable during July 19–21 (24/29, 37/41, and 26/29 mm, respectively) in the flood area of Henan Province, the daily precipitation was prone to be underestimated by ERA5 when the observed daily precipitation was above 150 mm (Figure 12). In contrast, the precipitation was prone to be overestimated by ERA5 when it was between 50 and

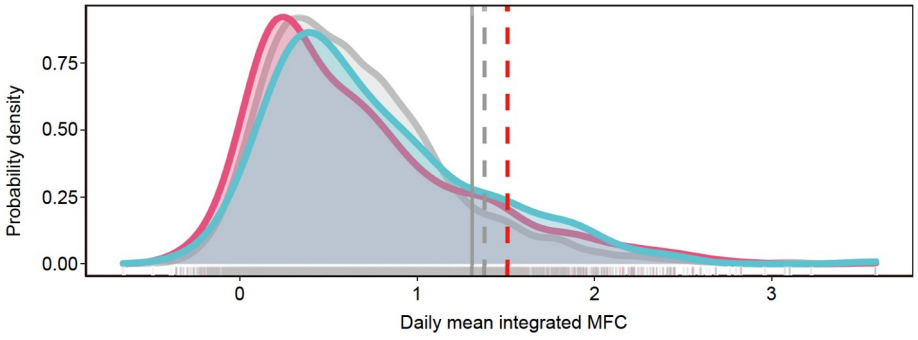

Figure 10 Probability density of the daily mean IMFC (unit: 10^{-3} kg m^{-2} s^{-1}) of the grid nearest to the EP event station for all summer days (gray line and shading), Type 8 circulation days (red line and shading), and Type 8-3 circulation days (blue line and shading). The vertical red and grey dashed lines represent the daily mean IMFC of the grid nearest the station with the maximum precipitation on July 20, 2021 and the maximum 3-day mean integrated IMFC in Henan Province and the adjacent regions in NC during July 19–July 21, 2021, respectively. The vertical solid lines represent the 90th percentile of the daily mean IMFC of the grid nearest to the EP event station for all summer days (grey).

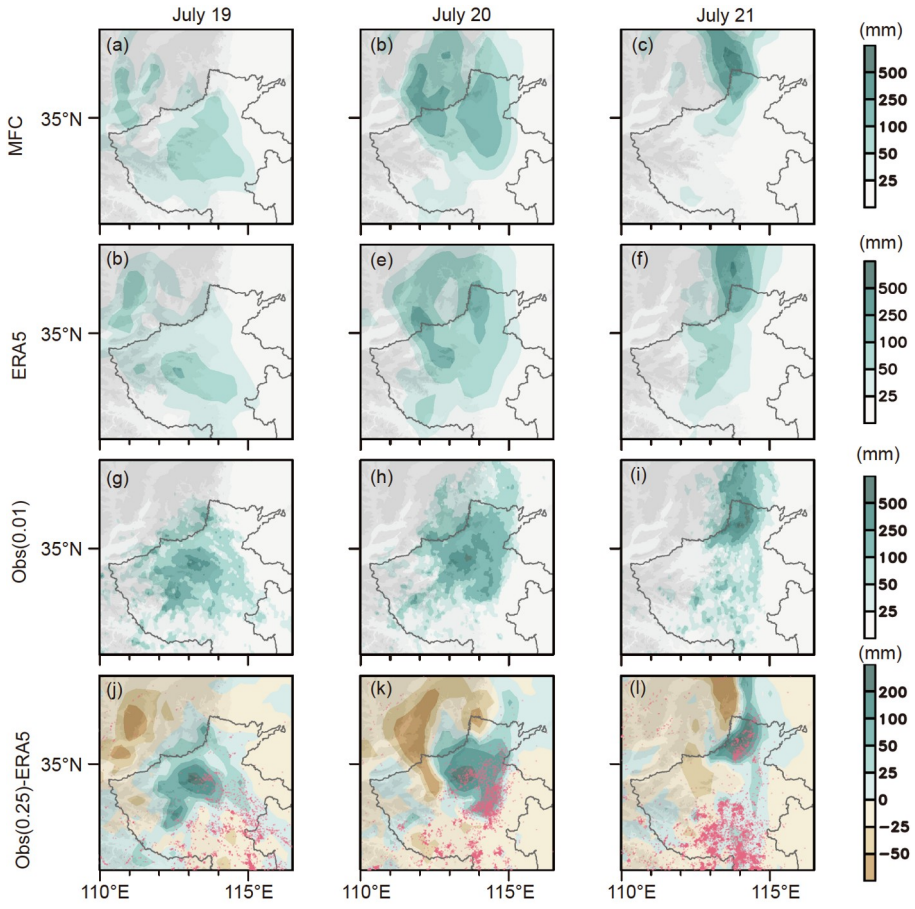

Figure 11 (a)–(c) The daily accumulated IMFC, (d)–(f) ERA5 daily precipitation, (g)–(i), the observed gridded precipitation with horizontal resolutions of 0.01°, and (j)–(l) the difference in daily precipitation between the observed gridded precipitation with a horizontal resolution of 0.25° and the ERA5 daily precipitation from July 19 to 21, 2021. Gray shading denotes the terrain height. Red dots denote the lightning locations.

100 mm (Figure 12). In addition, the precipitation estimated according to the daily IMFC in the grid nearest to Zhengzhou station on July 20, 2021 was 130 mm. The observed daily precipitation at that grid was 411 mm, such that the 130 mm amount estimated according to the daily IMFC represented 32% of the total precipitation in the grid nearest to Zhengzhou weather station on July 20, 2021. Meanwhile, at the 20 record-breaking stations from July 19 to July 21, the proportion of observed precipitation that could be represented by IMFC was 28%, 37% and 59% at the 25th, 50th and 75th percentile, respectively. Thus, the large-scale circulation alone does not explain the record-breaking precipitation for July 2021.

4. Discussion and conclusions

In this study, large-scale circulation patterns in East Asia associated with EP days in NC on summer days from 1979 to 2021 were analyzed using a clustering method, to identify the key dynamic factors underlying each circulation pattern. For "21·7", a further detailed circulation classification was conducted in NC and the three dominant circulation types directly promoting EP days were determined. The means for the 3 days during "21·7" and the same type of EP days in study periods were also compared to understand the extreme characteristics of the large-scale circulation related to the "21·7" flood.

The large-scale circulation pattern of "21·7" was characterized by a dipole pressure field, with low pressure in the southern part of China and the WPSH extending northward and westward to NC. Among the nine East Asian circulation types that occurred in summers from 1979 to 2021, "21·7" was found to occur under Type 8 circulation, which was not the majority circulation pattern and accounted for only 8% of summer days during the period examined. In contrast to other leading EP day circulation types with southwesterly winds in the low troposphere, 68% of Type 8 circulation days were associated with prevailing southeasterly winds in NC. Detailed circulation classification in NC under Type 8 showed that the spatial distributions of different EP events were determined by the location of the low in the dipole. The "21·7" event occurred under Type 8-3 circulation, which was characterized by a low in southwestern China extending

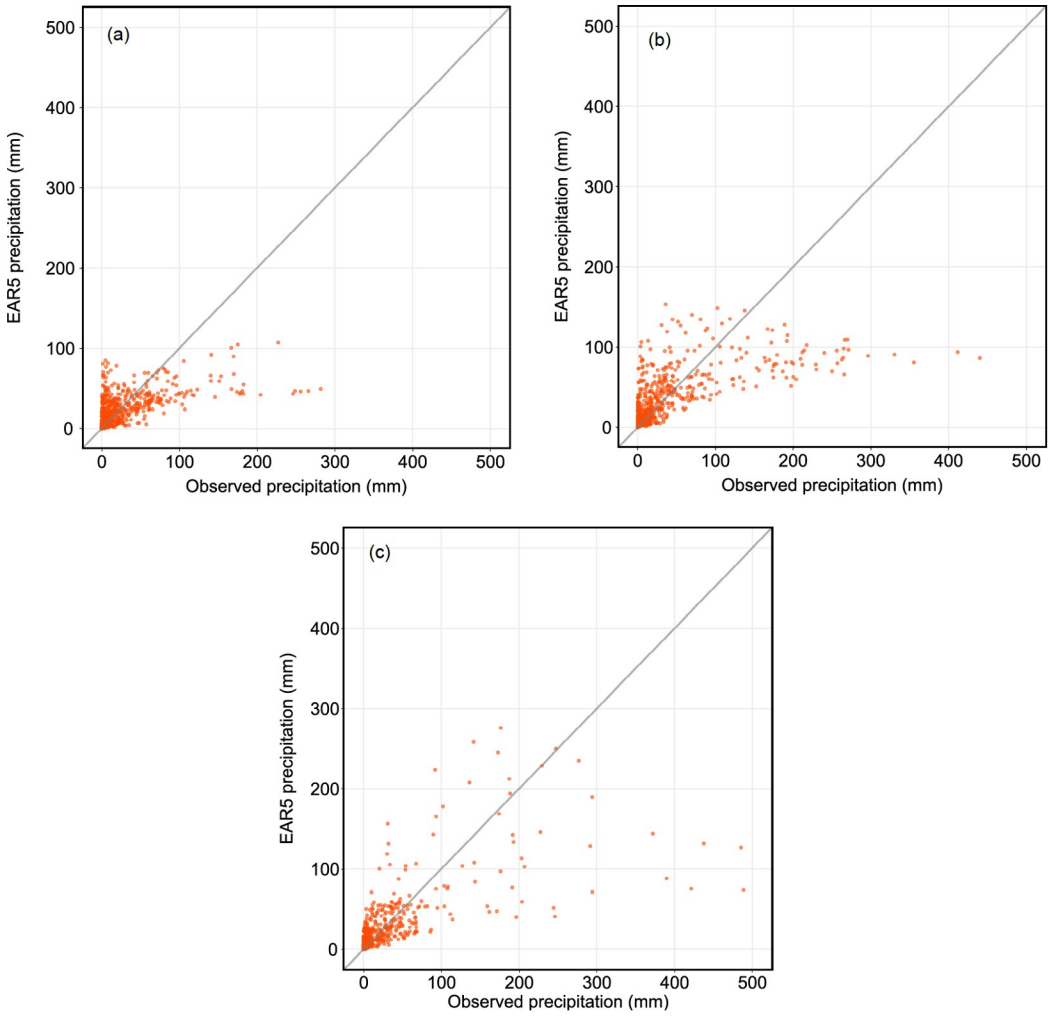

Figure 12 Scatter plots of the observed gridded precipitation with horizontal resolutions of 0.25° and the ERA5 daily precipitation on July 19 (a), July 20 (b), and July 21 (c), 2021.

northeastward to NC. Under this type of circulation, 23.1% were EP days and there were no dry days. Accordingly, under Type 8-3 circulation, more EP events occurred along the mountains in the NCP and more consecutive EP days were likely occur than under other circulation patterns

The EP days under Type 8 circulation involved both stronger low and high pressures in the dipole pressure field, forming a significantly stronger southerly wind from the East China Sea to parts of NC and bringing significantly more moisture. Additionally, a significantly stronger IMFC occurred in the NCP along the mountains in NC and the eastern part of NC, especially in the delta region, which was consistent with the spatial distribution of EP events under Type 8-3 circulation. Because Type 8-3 circulation accounted for only 21% of all Type 8 conditions, the frequency of "21·7"-like circulation was only 1.6%, which indicated that it was a very extreme circulation pattern. The interaction of the far northwestward-extending WPSH, the stronger low in southwestern NC and Typhoon In-fa in "21·7" led to it being in the top 8.7th percentile in IMFC of all EP events in the summer and the largest (second largest) in 3-day mean IMFC among 3 consecutive EP days under type 8 (all types) during the past 43 summers in NC. Better understanding of the large-scale circulation of EP days under Type 8 and Type 8-3 circulations could help prevent flood disasters in the cities along the mountains in the NCP.

Because Typhoon In-fa was underway in the East China Sea when the "21·7" occurred (Figure 8c), TC tracks under different circulation patterns were also investigated. The proportion of days accompanied by TC activities under Type 1–9 circulation were 46.8%, 16.7%, 64.1%, 30.3%, 33.4%, 50.8%, 46.3%, 77.2%, and 55.7%, respectively. The proportion of TC days in the EP days under Type 1–9 circulations were 50.8%, 6.7%, 57.1%, 30.0%, 30.7%, 46.2%, 38.1%, 72.5%, and 50.0% respectively. Type 8 circulation accounted for the highest proportion among all nine types of circulation on days with TCs. Interestingly, not all EP events under Type 8 circulation were associated with TC activities. For example, on July 16–17, 2018 there were urban waterlogging and landslide events in Beijing under Type 8 circu-

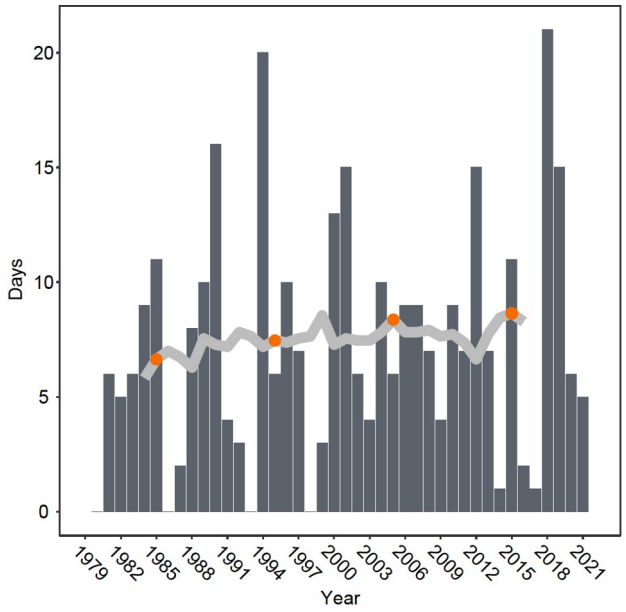

Figure 13 Annual days of Type 8 circulation. The gray line is the 11-year moving average. Red dots are the decadal mean days of Type 8 circulation in the 1980s, 1990s, 2000s, and 2010s.

lation. However, without TCs, strong southeasterly winds were observed during these two days (Figure not shown), indicating the importance of southerly winds to EP events under Type 8 circulation.

Although Type 8 circulation was a low-probability event, the number of days under this type of circulation exhibited large interannual variability (Figure 13). The days under Type 8 circulation followed a significant decadal increasing trend from the 1980s to 2010s, which was accompanied by the northward shift of the TC track (e.g., Studholme et al., 2022) over the past half century. The Type 8 circulation was associated with a wide monsoon trough in the South China Sea and abnormal northward and westward subtropical highs. Questions remain regarding what climate systems influence the interannual and interdecadal variability of days and EP days under Type 8 circulation, and how large-scale drivers will respond to the warming climate. Meanwhile whether the above simultaneous variations of Type 8 days and the TC tracks were determined by the variations of the same climate systems was remained to be explored.

The large-scale circulations and key dynamic factors integrated in the IMFC were identified and quantified, which would be helpful for weather forecasting and climate projections of EP days in NC. However, the IMFC calculated using ERA5 reanalysis data could explain 32% of the precipitation at the grid nearest to Zhengzhou weather station on July 20, 2021. In addition, these areas with severely underestimated precipitation by ERA5 were also accompanied by the most intense precipitation (>250 mm) and thunderstorms, indicating that mesoscale dynamic processes are also important for the intensity of EP. Further research will be required to clarify the mesoscale dynamic processes related to EP events under Type 8 and Type 8-3 circulations. Because large uncertainties remain in the resolution and detection of these mesoscale convective storms and in computing their associated precipitation in climate projections (e.g., Zhao, 2022), more research will also be required to determine how to link the mesoscale physics to large-scale climate dynamics in the projection of high-intensity EP events.

Acknowledgements *This work was supported by the Second Tibetan Plateau Scientific Expedition and Research Program (Grant No. 2019QZKK0105), the National Natural Science Foundation of China (Grant Nos. 42030607 & 41975001), the 2018 Open Research Program of the State Key Laboratory of Severe Weather (Grant No. 2018LASW-B17) and Forecaster Research Project of China Meteorological Administration (Grant No. CMAYBY2019-137).*

References

Banacos P C, Schultz D M. 2005. The use of moisture flux convergence in forecasting convective initiation: Historical and operational perspectives. Weather Forecast, 20: 351–366

Cao Y C, Zheng Y G, Sheng J, Lin Y J, Zhu W J, Zhang X W. 2020. Characteristics of three types of convective storms during the Beijing extreme precipitation event in 15–17 July 2018 (in Chinese). Meteorol Mon, 46: 885–897

Cressman G P. 1959. An operational objective analysis system. Mon Weather Rev, 87: 367–374

Davenport F V, Diffenbaugh N S. 2021. Using machine learning to analyze physical causes of climate change: A case study of U.S. Midwest extreme precipitation. Geophys Res Lett, 48: e93787

Ding Y H, Chan J C L. 2005. The East Asian summer monsoon: An overview. Meteorol Atmos Phys, 89: 117–142

Dowdy A J, Catto J L. 2017. Extreme weather caused by concurrent cyclone, front and thunderstorm occurrences. Sci Rep, 7: 40359

He Z W, Zhang Q H, Bai L Q, Meng Z Y. 2017. Characteristics of mesoscale convective systems in central East China and their reliance on atmospheric circulation patterns. Int J Climatol, 37: 3276–3290

Hersbach H, Bell B, Berrisford P, Hirahara S, Horányi A, Muñoz-Sabater J, Nicolas J, Peubey C, Radu R, Schepers D, Simmons A, Soci C, Abdalla S, Abellan X, Balsamo G, Bechtold P, Biavati G, Bidlot J, Bonavita M, Chiara G, Dahlgren P, Dee D, Diamantakis M, Dragani R, Flemming J, Forbes R, Fuentes M, Geer A, Haimberger L, Healy S, Hogan R J, Hólm E, Janisková M, Keeley S, Laloyaux P, Lopez P, Lupu C, Radnoti G, Rosnay P, Rozum I, Vamborg F, Villaume S, Thépaut J. 2020. The ERA5 global reanalysis. Q J R Meteorol Soc, 146: 1999–2049

Hu H B, Li J X, Zhang X. 2018. Lightning risk assessment at high spatial resolution at the residential sub-district scale: A case study in the Beijing metropolitan area. Geomatics Nat Hazards Risk, 9: 16–32

Huth R. 1993. An example of using obliquely rotated principal components to detect circulation types over Europe. Meteorol Z, 2: 285–293

Huth R. 1996a. An intercomparison of computer-assisted circulation classification methods. Int J Climatol, 16: 893–922

Huth R. 1996b. Properties of the circulation classification scheme based on the rotated principal component analysis. Meteorl Atmos Phys, 59: 217–233

Huth R. 2000. A circulation classification scheme applicable in GCM studies. Theor Appl Climatology, 67: 1–18

Li M X, Zhang Q H, Zhang F Q. 2016. Hail day frequency trends and associated atmospheric circulation patterns over China during 1960–2012. J Clim, 29: 7027–7044

Liao X N, Ni Y Q, He N, Song Q Y. 2013. Analysis of the synoptic-scale dynamic process causing the extreme moisture environment in the "7.21" heavy rain case (in Chinese). Acta Meteorol Sin, (6): 997–1011
Liu W B, Wang L, Chen D L, Tu K, Ruan C Q, Hu Z Y. 2016. Large-scale circulation classification and its links to observed precipitation in the eastern and central Tibetan Plateau. Clim Dyn, 46: 3481–3497
Liu Y, Wu G. 2004. Progress in the study on the formation of the summertime subtropical anticyclone. Adv Atmos Sci, 21: 322–342
Lu X, Yu H, Ying M, Zhao B K, Zhang S, Lin L M, Bai L N, Wan R J. 2021. Western North Pacific tropical cyclone database created by the China Meteorological Administration. Adv Atmos Sci, 38: 690–699
Mao J, Wang L, Lu C, Liu J, Li M, Tang G, Ji D, Zhang N, Wang Y. 2020. Meteorological mechanism for a large-scale persistent severe ozone pollution event over eastern China in 2017. J Environ Sci, 92: 187–199
Ng C P, Zhang Q, Li W, Zhou Z. 2022. Contribution of thunderstorms to changes in hourly extreme precipitation over China from 1980 to 2011. J Clim, 35: 4485–4498
Pan H, Chen G. 2019. Diurnal variations of precipitation over North China regulated by mountain-plains solenoid and boundary-layer inertial oscillation. Adv Atmos Sci, 36: 863–884
Shepherd T G. 2014. Atmospheric circulation as a source of uncertainty in climate change projections. Nat Geosci, 7: 703–708
Studholme J, Fedorov A V, Gulev S K, Emanuel K, Hodges K. 2022. Poleward expansion of tropical cyclone latitudes in warming climates. Nat Geosci, 15: 14–28
Sun W, Li J, Yu R C, Yuan W Y. 2015. Two major circulation structures leading to heavy summer rainfall over central North China. J Geophys Res-Atmos, 120: 4466–4482
Tao S Y. 1980. Heavy Rainfalls in China (in Chinese). Beijing: Science Press. 122
Wang B, Biasutti M, Byrne M P, Castro C, Chang C P, Cook K, Fu R, Grimm A M, Ha K J, Hendon H, Kitoh A, Krishnan R, Lee J Y, Li J, Liu J, Moise A, Pascale S, Roxy M K, Seth A, Sui C H, Turner A, Yang S, Yun K S, Zhang L, Zhou T. 2021. Monsoons Climate Change Assessment. Bull Am Meteorol Soc, 102: E1–E19
Xia R D, Zhang D L. 2019. An observational analysis of three extreme rainfall episodes of 19–20 July 2016 along the Taihang Mountains in North China. Mon Weather Rev, 147: 4199–4220
Xu J, Zhang Q, Bi B, Chen Y. 2022. Spring extreme precipitation days in North China and their reliance on atmospheric circulation patterns during 1979–2019. J Clim, 35: 2253–2267
Yao W, Zhang Y, Meng Q, Wang F, Lu W. 2012. A Comparison of the characteristics of total and cloud-to-ground lightning activities in hailstorms. Acta Meteorol Sin, 27: 282–293
Yin J F, Gu H D, Liang X D, Yu M, Sun J S, Xie Y X, Li F, Wu C. 2022. A possible dynamic mechanism for rapid production of the extreme hourly rainfall in Zhengzhou City on 20 July 2021. J Meteorol Res, 36: 1–20
Yin S, Li W, Chen D, Jeong J H, Guo W. 2011. Diurnal variations of summer precipitation in the Beijing area and the possible effect of topography and urbanization. Adv Atmos Sci, 28: 725–734
Ying M, Zhang W, Yu H, Lu X, Feng J, Fan Y, Zhu Y, Chen D. 2014. An overview of the China meteorological administration tropical cyclone database. J Atmos Ocean Tech, 31: 287–301
Zappa G, Hoskins B J, Shepherd T G. 2015. The dependence of wintertime Mediterranean precipitation on the atmospheric circulation response to climate change. Environ Res Lett, 10: 104012
Zhang D L, Lin Y, Zhao P, Yu X, Wang S, Kang H, Ding Y. 2013. The Beijing extreme rainfall of 21 July 2012: "Right results" but for wrong reasons. Geophys Res Lett, 40: 1426–1431
Zhao M. 2022. A study of AR-, TS-, and MCS-associated precipitation and extreme precipitation in present and warmer climates. J Clim, 35: 479–497
Zhao Y, Zhang Q, Du Y, Jiang M, Zhang J. 2013. Objective analysis of circulation extremes during the 21 July 2012 torrential rain in Beijing. Acta Meteorol Sin, 27: 626–635
Zhao Y, Xu X X, Li J, Zhang R, Kang Y Z, Huang W B, Xia Y, Liu D, Sun X Y. 2019. The large-scale circulation patterns responsible for extreme precipitation over the North China plain in midsummer. J Geophys Res-Atmos, 124: 12794–12809
Zhong L, Mu R, Zhang D, Zhao P, Zhang Z, Wang N. 2015. An observational analysis of warm-sector rainfall characteristics associated with the 21 July 2012 Beijing extreme rainfall event. J Geophys Res-Atmos, 120: 3274–3291
Zhou T J, Song F F, Lin R P, Chen X L, Chen X Y. 2013. The 2012 North China floods: Explaining an extreme rainfall event in the context of a long-term drying tendency. Bull Amer Meteorol Soc, 94: S49–S51
Zhou X, Sun J S, Zhang L N, Chen G J, Cao J, Ji B. 2020. Classification characteristics of continuous extreme rainfall events in North China (in Chinese). Acta Meteorolo Sin, 78: 761–777

(Responsible editor: Zhiyong MENG)